

*MODE EXCITATION AND AN EXPLANATION OF THE DIVERGENCE OF THE RADIATION
FROM A RUBY LASER*

A. M. LEONTOVICH and A. P. VEDUTA

P. N. Lebedev Physics Institute, Academy of Sciences, U.S.S.R.

Submitted to JETP editor July 12, 1963

J. Exptl. Theoret. Phys. (U.S.S.R.) 45, 71-79 (January, 1964)

Excitation of modes in each spike from a ruby laser with plane parallel mirrors has been investigated with a SFR-2M apparatus. From the near field pattern and the simultaneously obtained far field pattern it is concluded that the modes which are excited correspond to a spherical instead of a plane parallel resonator. This is explained by optical inhomogeneities in ruby and is the cause of the large divergence of the radiation beam from the laser. In moderate quality crystals additional divergence may be caused by scattering.

INTRODUCTION

IN optical masers, as in other generators of electromagnetic oscillations, the excitation takes the form of characteristic oscillations (modes) determined by the shape of the resonator, the distribution of the index of refraction and the boundary conditions.

The field amplitude distribution on the mirrors of the resonator corresponding to the excitation of a given mode has the form of a group of spots characteristic of that mode. The symmetry of the arrangement of spots is determined by the symmetry of the resonator and the type of oscillation. Knowing the near field pattern on the output mirrors of the resonator, one may find by Huygens' principle the directional distribution of the radiation in space (the far field pattern). It is the Fourier transform of the near field distribution on the mirror. Its character will depend on the mode of oscillation. Therefore, knowing experimentally the near field distribution on the mirror and comparing it with the far field pattern of the radiation, we can obtain information on the types of modes excited in the laser.

The distribution of radiation intensity on the end mirror of a laser corresponding to the excitation of particular modes has been studied for the gas laser^[1] and for ruby^[2-4]. The directional distribution of the radiation was not studied at the same time, nor was it compared with the near field pattern. This comparison is the subject of the present paper.

Mode excitation in the various types of resonators used in lasers has been treated theoretically in a series of papers^[5-8]. For example,

in a plane parallel resonator the field distribution u on the mirror has the form (for a rectangular mirror)^[5-7]

$$u = u_0 \cos k_x x \cos k_y y, \quad (1)$$

where $k_x = m\pi/D_x\beta_x$; $k_y = n\pi/D_y\beta_y$; D_x and D_y are the dimensions of the mirror in the directions of the corresponding axes; m and n are integers; and β_x and β_y are coefficients equal to or close to unity; for an open resonator (without side walls) these coefficients are complex. The radiation will propagate primarily in certain directions (in four directions in the case of a rectangular mirror) making an angle $\vartheta \approx \lambda(m^2/D_x^2 + n^2/D_y^2)^{1/2}$ to the mirror normal.

In a resonator with spherical mirrors having a radius of curvature R and a rectangular cross section and separated by a distance L modes will be excited^[8] with a near-field pattern of the following form (the z axis is along the axis of the resonator and the origin of coordinates is halfway between the mirrors):

$$u = u_0 \psi_m(x, z) \psi_n(y, z),$$

$$\psi_m(x, z) = H_m \left(2x \sqrt{\frac{\pi}{L_0 \lambda (1 + (2z/L_0)^2)}} \right) \times \exp \left[-\frac{2\pi x^2}{L_0 \lambda (1 + (2z/L_0)^2)} \right] \quad (2)$$

(the expression for $\psi_n(y, z)$ is similar), where $H_m(\xi)$ are the Chebyshev-Hermite polynomials of order m ; m and n are integers equal to the number of zeroes in the corresponding polynomials H_m and H_n ("the angular indices of the mode"); λ is the wavelength of the light; L_0 is the separation between the mirrors of a confocal resonator

(i.e., one for which $R = L_0$), which for $z \leq L/2$ has the same field distribution as the spherical resonator,

$$L_0 = \sqrt{2RL - L^2}. \quad (3)$$

The phase is constant over the mirror surfaces; at other points in space the surfaces of constant phase are spheres with radii of curvature $\geq L_0$ and centers of curvature lying on the axis of the resonator.

From (2) it is clear that the field distribution has the same form for various values of z ; i.e., for various separations z from the center of the resonator the field distribution is geometrically similar and changes only in size. The active region is smallest in size in the plane $z = 0$, where the surface of constant phase is a plane. In this plane the size of the active region has dimension D (measured to an intensity 0.03 times the maximum):

$$D = \kappa_m \sqrt{L_0 \lambda / \pi}, \quad (4)$$

where the κ_m are coefficients whose values are given in Table I. The far-field pattern of the radiation is the Fourier transform of the field distribution in the plane $z = 0$ and is similar in form to the near-field pattern. This is because the modes of a spherical resonator are described by functions (2) which are eigenfunctions of the Fourier transformation.

Thus the radiation corresponding to a mode with index m propagates with a divergence varying widely with m , viz: a total divergence (to 0.03 times maximum intensity):

$$\varphi = 2 \sqrt{\lambda / L_0 \pi} \kappa_m = (2\lambda / D) (\kappa_m^2 / \pi). \quad (5)$$

The frequency of the excited mode satisfies the following relations:

$$\frac{v}{c} = \left(\frac{v}{c}\right)_{\text{ax}} + \frac{m+n}{4L} \left(1 - \frac{4}{\pi} \chi\right),$$

$$\left(\frac{v}{c}\right)_{\text{ax}} = \frac{q}{2L} + \frac{1}{4L} \left(1 - \frac{4}{\pi} \chi\right), \quad \tan \chi = \frac{L_0 - L}{L_0 + L}, \quad (6)$$

where q is an integer (the "axial index" of the

mode). If $R \gg L$ (or $L_0 \gg L$), we have approximately

$$\frac{v}{c} = \left(\frac{v}{c}\right)_{\text{ax}} + (m+n) \frac{2}{\pi L_0} = \left(\frac{v}{c}\right)_{\text{ax}} + (m+n) \frac{1}{\pi} \sqrt{\frac{2}{RL}}. \quad (7)$$

THE EXPERIMENT

As is well known the output of a ruby laser occurs in pulses (spikes). Within a given spike several modes are excited having the same angular but different axial indices^[9]. To study mode excitation in individual spikes lasting 0.3–0.7 sec, a fast SFR-2M framing camera was used in the "time magnifier" mode (i.e., showing sequential development). In order to get simultaneous pictures of the near and far field patterns using a single SFR camera, the laser beam was sent through a beam splitter. The separate beams then passed through different optical systems (Fig. 1) and fell on two openings in a special entrance diaphragm in the SFR-2M. This made it possible to record the two field distributions simultaneously¹⁾. The cross sections of the beams in the plane of the diaphragm were several times smaller than the size of the diaphragm, so that no vignetting of the laser light occurred. Each pair of exposures on the film corresponded to the si-

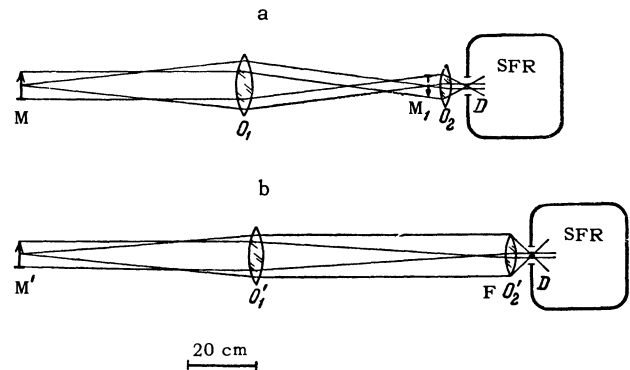


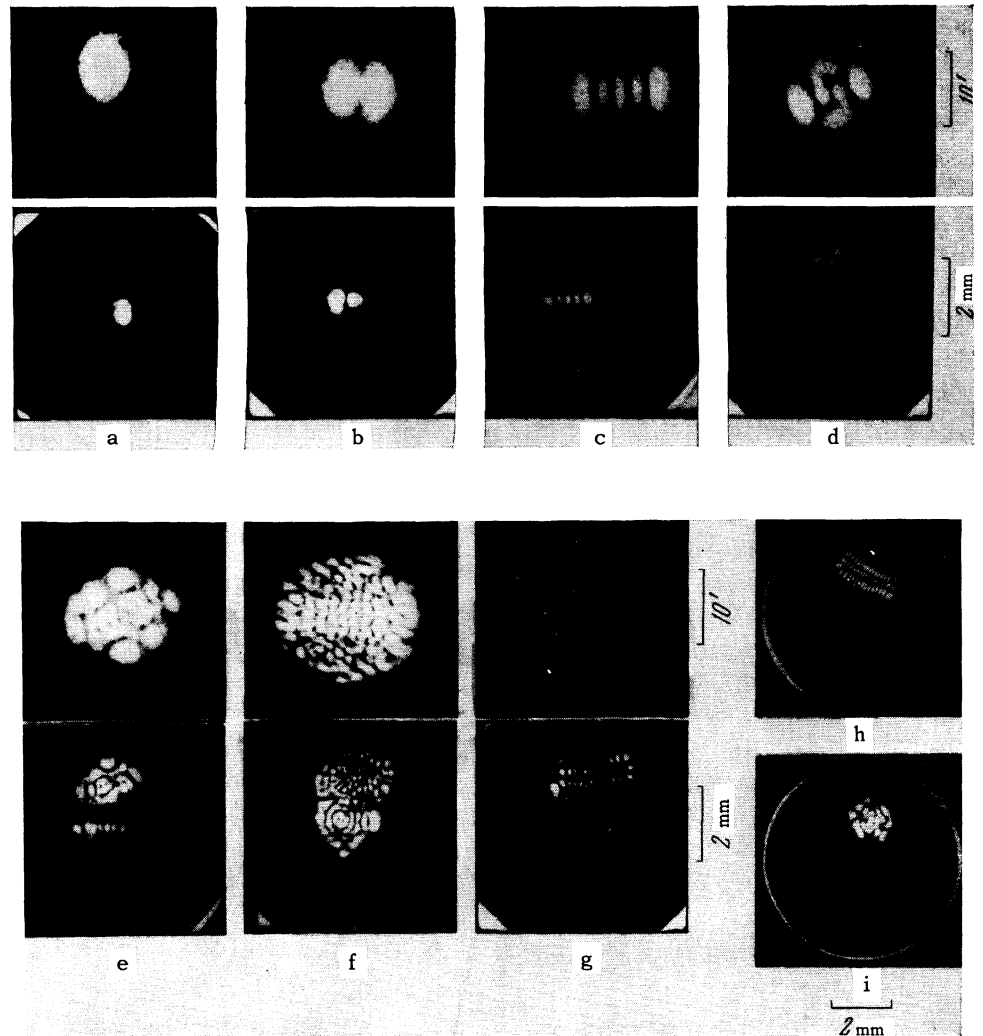
FIG. 1. Optical system: a—for photographing the near field pattern on the mirror (M—end mirror of the resonator, O_1 and O_2 —lenses with focal lengths $f_1 = 30$ cm and $f_2 = 5$ cm, M_1 —first image of the mirror, $M_1 O_2 = f_2$, D—diaphragm); b—for photographing the far field pattern of the radiation (M' —end mirror of the resonator, O'_1 and O'_2 —lenses with focal lengths $f'_1 = 70$ cm and $f'_2 = 5$ cm, D—diaphragm, and $M' O'_1 = O' F = f'_1$, $F O'_2 = f'_2$).

Table I

m	κ_m	m	κ_m
0	1.86	8	4.73
1	2.51	9	4.97
2	2.97	10	5.18
3	3.35	11	5.38
4	3.68	12	5.57
5	3.98	13	5.76
6	4.25	14	5.93
7	4.50		

¹⁾In the SFR-2M camera as it left the factory, the entrance aperture consisted of two (or four) rectangular holes, moveable with respect to each other. Our diaphragm consisted of two rectangular holes arranged one over the other.

FIG. 2. Simultaneous near field (below) and far field (above) patterns for different spikes. The mirrors are on the ends of the crystal. The length of the crystal is 5 cm (the outline of the end face is visible in the pictures). a - TEM_{00} mode, b - TEM_{01} , c - TEM_{04} , d-h - more complicated modes; i - $TEM_{2,14}$ (h and i show only the near field pattern on the mirror).



multaneous recording of the near field pattern on an end mirror and the far field pattern (directional distribution) during one or several spikes, depending on the exposure time. The exposure time of a frame could be varied from 1.6 to 12 μsec . by varying the rate of rotation of the mirror in the camera. The interval between successive frames was twice the exposure time.

The laser employed a ruby crystal in the form of a polished cylinder of length $l = 50$ mm, and diameter about 7 mm, having plane parallel ends. The optic axis c of the crystal was perpendicular to the axis of the rod, hence the polarization of the laser output was always the same (the electric vector was perpendicular to the z axis^[10]). Experiments were made both with the mirrors on the ends of the crystal and with external plane mirrors. Since the pump energy only slightly exceeded the laser threshold, focusing of the pump light by the cylindrical walls of the ruby rod^[11] caused only the central region of the crystal to be excited.

RESULTS

We show in Fig. 2 individual exposures which record simultaneously the far field radiation pattern and the near field pattern on the mirror. Different frames, corresponding to different spikes, exhibit different patterns—from a single, simple spot to a complicated distribution of a large number of spots. A single mode is characterized by a pattern exhibiting to some degree a symmetric distribution of spots. More exactly, such a distribution corresponds to the simultaneous excitation of several modes which have the same angular index but different axial indices^[9]. For brevity we will speak of a single mode in this case.

We ascertained that the different spots of such a pattern belonged to a single mode, i.e., were mutually coherent, by obtaining interference between the various spots using apparatus described in^[9]. This experiment was done by superposing two images of the intensity distribution (the direct

image and a rotated image); the resulting picture showed vertical interference bands (Fig. 3).

It is clear from the exposures in Fig. 2 that the near and far field patterns are similar. It follows that the modes excited in the laser correspond to a spherical cavity rather than to a plane parallel cavity. The general form of the near-field patterns on the mirror also reminds one of patterns obtained from lasers with spherical mirrors (cf. for example [1]). Measurements were made of the relative separations between minima in the intensity distributions characterizing several modes (for example modes like those shown in Figs. 2c, g, i). It was found that the minima were not equidistant as they should be for a plane parallel resonator [Eq. (1)], whereas their arrangement agrees with the distribution of zeroes of the functions ψ_m (calculated in [12]).

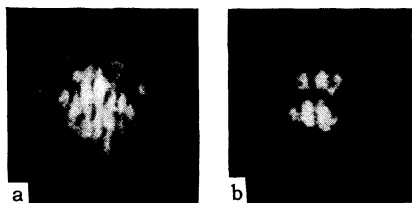


FIG. 3. Interference between two images of the far field pattern, one rotated with respect to the other around the vertical axis (for two different spikes).

Moreover it follows from (5) that the total angular divergence of the beam φ and the size of the excited region D for a mode in a plane where the wave front is plane (and because of the boundary conditions the plane of the mirror should be a surface of constant phase) are related by the relationship $\sqrt{\varphi D} = \kappa_m \sqrt{2\lambda/\pi}$. Using the pictures of several modes²⁾, measurements were made of the total beam divergence φ and the size of the excited region D of the mode on the mirror (for various mirror separations and various crystals), and the values of $\sqrt{\varphi D}$ were compared with the calculated values. The results of this comparison are shown in Table II. As can be seen from the table, the experimental and theoretical values differ by no more than 3–4%, which is very good agreement under our experimental conditions. Also shown in the table are the values of L_0 —the separation between mirrors of the corresponding

²⁾Since the theory^[8] was worked out only for modes with rectangular symmetry, we selected only this type of modes from the great diversity of modes observed in these experiments.

confocal resonator calculated from the formula $L_0 = 2D/\varphi$ [which follows from (4) and (5)]. The reasons for the excitation of modes corresponding to a spherical resonator will be discussed in the following section.

The sequence in which the various modes were excited was followed throughout the length of the pumping pulse. Near the beginning of laser action, in the initial spikes, simple modes are excited (Figs. 2a and b). These modes are almost purely axial and are excited in a small region of the crystal of dimension $D \approx 0.3$ mm. Following this the extent of the laser action region grows (in our experiments to 2–3 mm), and more complex modes, which differ markedly from purely axial, are excited (Figs. 2d, e, and f). At the same time one observes two (and sometimes more) groups of spots on the mirror; each group of spots has a symmetric arrangement. The far field pattern is similarly observed to be a superposition of two patterns. This means that there are two (or correspondingly more) regions in the crystal where modes are excited.

It was also observed that increasing the separation between the external mirrors L led to the excitation of simpler modes.

The deviation in frequency of an excited non-axial mode from the frequency of the corresponding purely axial mode can be calculated from (7). It is interesting to compare this quantity with the frequency difference c/L between adjacent axial modes:

$$\frac{\nu - \nu_{ax}}{c/2L} = \frac{4(m+n)L}{\pi L_0}$$

For the modes listed in Table II this ratio can reach two.

The near field patterns on the two opposite mirrors were investigated simultaneously. Pictures taken with the SFR camera are shown in Fig. 4. It is clear that the patterns on both mirrors are identical (the small difference in scale and the rotation of one of the images are due to the fact that different optical systems were used in photographing the two ends).

The orientation of the spot patterns relative to the crystallographic c axis was found to be random; no correlation was observed between the symmetry of the spot patterns and the orientation of the optic axis.

In some crystals, and sometimes in the same crystal but with variation of the region of laser action, the radiation distribution exhibited a more complicated character. In these cases the pictures corresponding to modes were accompanied

Table II. Beam divergence φ , dimension D of mode excitation region, comparison with theory, and magnitude of inhomogeneity δ for different modes, different crystals (crystal length $l = 5$ cm), and different distances between outer mirrors L

m	φ	D , mm	$\sqrt{\varphi D} \cdot 10^2$, experiment	$\sqrt{\frac{2\lambda}{\pi}} \kappa m \cdot 10^2$, calculated	L_0 , cm	f , cm	δ , μ
Crystal A $L = 5$ cm							
0	6.35'	0.80	1.32	1.24	73	156	0.8
2	9.6'	0.96	1.78	1.98	58	100	1.2
4	12.3'	1.34	2.38	2.45	64	120	1.0
6	15.7'	1.60	2.94	2.83	60	107	1.2
12	16.8'	2.27	3.62	3.71	80	180	0.7
Crystal B $L = 21$ cm							
2	5.7'	1.95	1.96	1.98	195	390	0.3
6	8.6'	2.30	2.61	2.83	155	250	0.5
10	12.6'	2.70	3.42	3.44	125	170	0.7
Crystal C $L = 30$ cm							
{0	4.6'	0.96	1.24	1.24	120	120	1.0
{1	4.4'	1.35	1.43	1.67	180	250	0.5
{1	4.4'	1.51	1.50	1.67	200	310	0.4
{3	8.4'	1.62	2.23	2.23	112	110	1.1
13	11.5'	3.76	3.87	3.83	185	270	0.5
Crystal D $L = 30$ cm							
{0	3.22'	1.04	1.07	1.24	185	270	0.45
{1	4.33'	1.59	1.54	1.67	215	355	0.25
5	10.1'	2.32	2.85	2.65	135	145	0.8
Crystal B $L = 49$ cm							
1	4.7'	1.50	1.55	1.67	190	220	0.6
2	4.4'	1.52	1.63	1.98	200	240	0.5

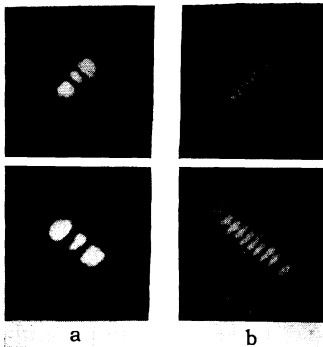


FIG. 4. Simultaneous output distributions on opposite mirrors (for two different spikes).

by a complicated background and a large number of irregularly distributed spots (Fig. 5). Evidently the complex background is due to the scattering of light by foreign inclusions, and the extra spots (light patches) are due to reflections at boundaries between microcrystals approximately parallel to the rod axis. This scattering further increases the divergence of the laser beam. The mirrors of the cavity act as a Fabry-Perot interferometer

for this scattered light and cause it to appear primarily at angles ϑ to the axis which satisfy the conditions for the Fabry-Perot interferometer^[13]. When the mirrors are located on the ends of the crystal these conditions have the form

$$2L\mu \cos \vartheta' = p\lambda, \quad \sin \vartheta = \mu \sin \vartheta', \quad (8)$$

where μ is the index of refraction of ruby, p is an integer, and ϑ' is the angle of the light beam with respect to the axis inside the ruby. In this case the far field radiation pattern will have the form of rings satisfying conditions (8); as is well known, these rings have been observed experimentally (cf. for example^[13,14]).

DISCUSSION

It may be assumed that the excitation of modes corresponding to a spherical cavity is due in our case to the optical inhomogeneities of a real crystal. We assume that the variation of the refractive

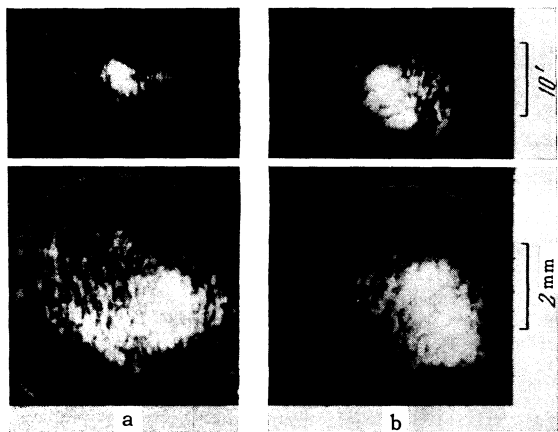


FIG. 5. Radiation patterns in crystals with scattering. Below, near field pattern on a mirror; above, the far field pattern. Mirror separation 25 cm.

index within an optical inhomogeneity is such that the length of the optical path parallel to the axis of the rod and going through the center of the inhomogeneity is greater by an amount δ than the optical path length at a distance a from the center of the inhomogeneity. To first approximation δ depends quadratically on a . It was shown by Hercher^[15] that laser action occurs initially near such regions. Thus the effect of the inhomogeneity is the same as that of a positive lens with a focal length $f = a^2/2\delta$.

If a lens with focal length f is placed alongside one of the mirrors (which are separated by a distance L) inside a plane parallel resonator, the resonator will be equivalent to a spherical resonator with mirror separation $2L$ and radius of curvature of the mirrors f . In this case the corresponding value of L_0 , as given by (3), is $L_0 = \sqrt{4Lf - 4Lf^2}$. If the lens is placed at the center of the resonator, it will be equivalent to a spherical cavity with a mirror separation L and a radius of curvature of the mirrors $2f$. In this case $L_0 = \sqrt{4Lf - L^2}$. In the general case

$$L_0 = \sqrt{4Lf - \alpha^2 L^2}, \quad 1 \leq \alpha \leq 2. \quad (9)$$

From experiment we know the values of L_0 for the modes excited (Table II). The quantity a can be set equal to half the size of the laser-action region at the mirror; it is clear from Fig. 2 that $a \approx 1.5$ mm. Knowing L_0 and a we can use (9) to calculate the effective focal length f of the inhomogeneity and also the quantity δ . These values are given in Table II. It was assumed that $\alpha \approx 1.4$ for the cases where L was 5, 21, and 30 cm and $\alpha = 2$ for $L = 49$ cm, in accordance with the position of the crystal inside the resonator. It is clear from Table II that the inhomogeneities which give

rise to the excitation of spherical modes are quite small, no larger than 1.5μ . We examined the internal optical inhomogeneity of our crystals by means of a Michelson interferometer, as was done in [15], and found that the variation in optical length of the crystals was not more than $1-1.5 \mu$ for a 2-3 mm cross-section. Thus we have good agreement.

In addition to the inhomogeneities it already possesses, the crystal may become inhomogeneous during the course of laser action due to uneven heating by the pump light. The focusing of the pump light by the cylindrical surface of the ruby [11] and the better heat transfer at the surface of the crystal cause the central portion of the crystal to be heated more strongly than the peripheral region. In ruby the index of refraction increases with temperature [17], and hence the inhomogeneity produced by heating the crystal will be similar to a positive lens which, as was discussed above, promotes laser action.

We assume that all of the pump light is absorbed only by chromium atoms and that the fraction of pump light absorbed in each of the three absorption bands of chromium is the same. Then, taking account of the fact that the luminescence quantum efficiency of ruby is 70% [16], we find that the luminescence energy yield due to excitation by pump light is $\approx 20\%$. The remaining 80% is converted into heat. Near threshold slightly more than one half the chromium atoms are in the excited state. Knowing the concentration of chromium atoms N and the heat capacity of ruby, $C = 3$ joules/cm³ deg, we find that the temperature of ruby near threshold increases by an amount $\Delta T = C^{-1}(80/20)h\nu \cdot N/2$, where ν is the transition frequency. This quantity turns out to be about $0.5-1^\circ$. Taking $\partial L/\partial T$ and $\partial \mu/\partial T$ from [17] we find that the optical length of the resonator varies due to heating by no more than 1.5μ . The inhomogeneities δ due to uneven heating cannot exceed this amount.

Thus the reason for the excitation of modes corresponding to a spherical resonator is the presence of optical inhomogeneities in the crystal. These may either be present in the crystal from the time of its growth, or may arise during laser action by uneven heating due to the pump light. At present there is not enough experimental data to indicate which type of inhomogeneity is more important.

It is clear from Table II that the magnitude of δ is different for different modes. It is possible that differences in thermal inhomogeneity are responsible for this. It should also be kept in mind however that different modes are excited in differ-

ent regions of the crystal having, probably, different values of the quantity δ .

It is clear from the pictures that the modes excited in different spikes have different types of symmetry. Clearly the character of the inhomogeneity and its symmetry determine the symmetry properties of the excited modes. For example if the optical effect of an inhomogeneity is similar to an astigmatic lens with different effective focal lengths f in two perpendicular planes, then a mode will be excited having rectangular symmetry (this type of mode occurs in Table II). For several such modes the values φ and D were measured in perpendicular directions (these quantities, belonging to a single mode, are connected in Table II by curly brackets). It is clear from the table that the obtained quantities f and δ are in fact different.

The sequence of mode excitation during the pumping pulse may be explained as follows. It follows from (4) that the region of mode excitation grows in size with increasing angular complexity of the mode, i.e., with increasing m . Near the beginning of laser action the region of population inversion in the crystal is small and therefore only low order modes can be excited, modes with small m . As the pump power increases the region of laser action grows and higher order modes can be excited, as is indeed observed.

Thus the general picture of mode excitation in lasers with plane parallel mirrors is as follows. Optical inhomogeneities, whether present in the crystal or due to uneven heating by pump light, distort the resonator and excite modes corresponding to a spherical resonator³⁾. In the latter type of resonator the region of mode excitation is very much compressed [see Eq. (4)], and the separation between neighboring maxima d in the near-field pattern on the mirrors decreases to about 0.2 mm. At the same time the beam divergence φ due to diffraction and given by the formula $\varphi \approx 2\lambda/d$ will be rather large (as large as 20'). This explains the large divergence of the output beam of a ruby laser with plane mirrors⁴⁾. When a spherical resonator is used it is the shape of the mirrors which determines the excitation of the modes and the optical inhomogeneities have the role of small perturbations.

³⁾The excitation of modes corresponding to a spherical cavity also explains the relative insensitivity of the laser characteristics to mirror adjustment observed in [18], since adjustment requirements for the spherical cavity are much less than for the plane parallel case.

⁴⁾A similar conclusion was also reached recently in [19].

The exact formula for the total beam divergence has the form

$$\varphi = 2\sqrt{\lambda/\pi\kappa_m} (4Lf - \alpha^2 L^2)^{-1/4}. \quad (10)$$

In this formula the quantity f characterizing the inhomogeneity occurs in a fourth root. This explains why laser beam divergence varies very little from crystal to crystal. Similarly Eq. (10) gives a stronger dependence of φ on the separation between the mirrors L than is experimentally observed; the divergence decreases with increasing L . Moreover it follows from (4) that the region where modes are excited increases with increasing L , and hence for a given size of excitation region lower modes are excited for large L than for small L ; this too is observed experimentally.

From the same equation (4) we can find the maximum size of an inhomogeneity for which the resonator will still function as a plane parallel cavity. For this it is clearly necessary that the size of the excited region D for an axial mode ($m = 0$) be larger than the diameter of the crystal D_0 . Combining (4) and (3), we obtain

$$f > \frac{\pi^2 D_0^4}{4\lambda^2 \kappa_0^4 L} + \frac{\alpha^2}{4} L.$$

Putting $D_0 = 5$ mm, $L = 10$ cm, $\alpha = 1$, and $\kappa_0 = 1.86$ we find that f must be $> 2.55 \times 10^5$ cm. This corresponds to $\delta = 1.2 \times 10^{-7}$ cm. At present it is impossible to obtain ruby crystals of this degree of uniformity; moreover it would be useless to do so since the inhomogeneities due to heating of the crystal during laser action are always larger.

We may thus draw the following conclusion. The beam divergence of a ruby laser is due to the excitation of modes corresponding to a spherical resonator, which in turn is due to optical inhomogeneities in the ruby. In crystals of medium quality this divergence is further increased by scattering in the crystals.

The authors express sincere thanks to M. D. Galanin for discussions and constant interest in the work and to L. A. Vainshtein for discussions.

¹⁾D. R. Herriott, J. Opt. Soc. Amer. **52**, 31 (1962). H. Kogelnik and W. W. Rigrod, Proc. IRE **50**, 220 (1962).

²⁾E. S. Dayhoff, Proc. IRE **50**, 1684 (1962).

³⁾V. Evtuhov and J. K. Neeland, Appl. Optics **1**, 517 (1962).

⁴⁾T. P. Hughes and K. Young, Nature **196**, 4852, 332 (1962).

⁵⁾A. L. Schawlow and C. H. Townes, Phys. Rev. **112**, 1940 (1958).

- ⁶A. G. Fox and T. Li, *Bell. Syst. Techn. J.* **40**, 453 (1961).
- ⁷L. A. Vainšteĭn, *JETP* **44**, 1050 (1963), *Soviet Phys. JETP* **17**, 709 (1963).
- ⁸G. D. Boyd and J. P. Gordon, *Bell. Syst. Techn. J.* **40**, 489 (1961).
- ⁹V. V. Korobkin and A. M. Leontovich, *JETP* **44**, 1847 (1963), *Soviet Phys. JETP* **17**, 1242 (1963).
- ¹⁰D. F. Nelson and R. J. Collins, *Advances in Quantum Electronics*, ed. J. Singer, 1961, p. 79.
- ¹¹Devlin, McKenna, May, and Schawlow, *Appl. Optics* **1**, 11 (1962).
- ¹²R. E. Greenwood and J. J. Miller, *Bull. Amer. Math. Soc.* **54**, 765 (1948).
- ¹³J. D. Abella and C. H. Townes, *Nature* **192**, 4806, 957 (1961).
- ¹⁴Galanin, Leontovich, and Chizhikova, *JETP* **43**, 347 (1962), *Soviet Phys. JETP* **16**, 249 (1963).
- ¹⁵M. Hercher, *Appl. Optics* **1**, 665 (1962).
- ¹⁶E. E. Bukke and Z. L. Morgenshtern, *Optika i Spektroskopiya* **14**, 687 (1963).
- ¹⁷M. A. Jeppesen, *J. Opt. Soc. Amer.* **48**, 629 (1958).
- ¹⁸J. F. Ready and D. L. Hardwick, *Proc. IRE* **50**, 2483 (1962).
- ¹⁹V. Evtuhov and J. K. Neeland, *Appl. Optics* **2**, 319 (1963).

Translated by J. A. Armstrong
10